Food Chemistry: X 22 (2024) 101346

Contents lists available at ScienceDirect

Food Chemistry: X

journal homepage: www.sciencedirect.com/journal/food-chemistry-x

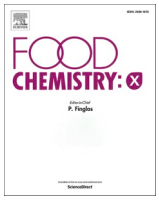

Physicochemical properties of starches from sweet potato root tubers grown in natural high and low temperature soils

Laiquan Shi [a,b,1], Ke Guo [a,c,1], Xin Xu [a,b], Lingshang Lin [a], Xiaofeng Bian [c], Cunxu Wei [a,b,*]

[a] Key Laboratory of Crop Genetics and Physiology of Jiangsu Province / Jiangsu Key Laboratory of Crop Genomics and Molecular Breeding, Yangzhou University, Yangzhou 225009, China
[b] Co-Innovation Center for Modern Production Technology of Grain Crops of Jiangsu Province / Joint International Research Laboratory of Agriculture & Agri-Product Safety of the Ministry of Education, Yangzhou University, Yangzhou 225009, China
[c] Institute of Food Crops, Jiangsu Academy of Agricultural Sciences, Nanjing 210014, China

ARTICLE INFO

Keywords:
Molecular structure
Crystalline structure
Thermal properties
Enzyme hydrolysis
Principal component analysis

ABSTRACT

Three sweet potato varieties grew in natural high temperature (HT) and low temperature (LT) field soils. Their starch physicochemical properties were affected similarly by HT and LT soils. Compared with LT soil, HT soil induced the increases of granule size D[4,3] from 18.0–18.7 to 19.9–21.8 μm and amylopectin average branch-chain length from 21.9–23.1 to 24.1–24.7 DP. Starches from root tubers grown in HT and LT soils exhibited C_A- and C_C-type XRD pattern, respectively. Starches from root tubers grown in HT soil exhibited stronger lamellar peak intensities (366.8–432.0) and higher gelatinization peak temperature (72.0–76.8 °C) than those (176.2–260.5, 56.4–63.4 °C) in LT soil. Native starches from root tubers grown in LT soil were hydrolyzed more easily (hydrolysis rate coefficient 0.227–0.282 h^{-1}) by amylase than those (0.120–0.163 h^{-1}) in HT soil. The principal component analysis exhibited that starches from root tubers grown in HT and LT soils had significantly different physicochemical properties.

1. Introduction

Sweet potato (*Ipomoea batatas*), a major starchy crop, contains many colored-fleshed root tubers with different contents of phenolic compounds and pigments (Alam, 2021). The white-, purple- and yellow-fleshed dry root tubers have over 60%, 53% and 45% starch, respectively (Guo et al., 2019). Sweet potato starch not only can be used to produce noodles and vermicelli, but also is a main raw material in food and nonfood industries (Song et al., 2021; Truong, Avula, Pecota, & Yencho, 2018). Starch is semicrystalline granules mainly consisted of amylose and amylopectin, and its molecular components and physicochemical properties determine the qualities of starchy crops (Emmambux & Taylor, 2013; Pérez, Baldwin, & Gallant, 2009; Song et al., 2021). Therefore, it is important to investigate the factors influencing starch properties of sweet potato for breeders, farmers and starch users.

Starch properties are affected by growth temperature during starch formation and accumulation in many plants. Previous studies are mainly focused on cereal crops, especially on rice (Fan et al., 2020; Tu et al., 2023; Yang, Wei, Lu, & Lu, 2021). The effects of growth temperature on starches from root tuber crops are few due to the difficulty in regulating soil temperature. Noda, Kobayashi, and Suda (2001) and Genkina et al.

Abbreviations: AAC, apparent amylose content; AAG, *Aspergillus* niger amyloglucosidase; ACL, average branch-chain length; AM, amylose molecule; AP_L, amylopectin long branch-chain; AP_S, amylopectin short branch-chain; BV, blue value; ΔH, gelatinization enthalpy; ΔT, gelatinization temperature range; D, lamellar repeat distance; DSC, differential scanning calorimetry; FACE, fluorophore-assisted capillary electrophoresis; GBSSI, granule-bound starch synthase I; GPC, gel permeation chromatography; HT, high temperature; k, hydrolysis rate coefficient; LT, low temperature; MRDM, mean relative deviation modulus; NZS1, Ningzishu 1; PCA, principal component analysis; PI, peak intensity; PPA, porcine pancreatic α-amylase; RC, relative crystallinity; RDS, rapidly digestible starch; RS, resistant starch; SAXS, small-angle X-ray scattering; SBE, starch branching enzyme; SDS, slowly digestible starch; SS, soluble starch synthase; SS16, Shushu 16; SS28, Sushu 28; SUMSQ, sum of squares of residuals; Tc, gelatinization conclusion temperature; To, gelatinization onset temperature; Tp, gelatinization peak temperature; XRD, X-ray diffraction.

* Corresponding author at: Key Laboratory of Crop Genetics and Physiology of Jiangsu Province / Jiangsu Key Laboratory of Crop Genomics and Molecular Breeding, Yangzhou University, Yangzhou 225009, China.
E-mail addresses: 007520@yzu.edu.cn (L. Lin), cxwei@yzu.edu.cn (C. Wei).
[1] Shi L. and Guo K. contributed equally to this work.

https://doi.org/10.1016/j.fochx.2024.101346
Received 7 January 2024; Received in revised form 15 March 2024; Accepted 31 March 2024
Available online 3 April 2024

(2003) planted two sweet potato cultivars in a temperature-controlled greenhouse in which soil temperature is maintained at four levels of 15, 21, 27 or 33 °C and air temperature is at 28 °C day / 23 °C night. The soil temperature during root tuber development has significant effects on starch properties (Noda et al., 2001). Starch exhibited C-type X-ray diffraction (XRD) pattern in root tuber grown in 21 °C soil, and shifts to A-type in 33 °C soil and C_B-type in 15 °C soil (Genkina et al., 2003). In recent, Guo et al. (2022) planted one sweet potato variety in growth chambers with the same soil and air temperatures. Three growth chambers have the identical humidity and light time/intensity, but each have constant temperature at 21, 25 and 28 °C. They found that amylose content has no significant variation among different growth temperatures, but amylopectin synthesis-related enzyme genes have different expressions among different growth temperatures, resulting in different amylopectin structures and crystalline structures.

Sweet potato is widely planted in tropical, subtropical and temperate countries and harvested at different dates or seasons (Alam, 2021). The root tubers planted and harvested at different dates are subjected to different temperature soils during their development (Noda, Takahata, Sato, Ikoma, & Mochida, 1997). The field soil temperature also varies within a day. Therefore, in production practice, it is more meaningful to investigate the effects of natural field soil temperature on starch properties than those of constant temperature in greenhouse and growth chamber. The study of Noda et al. (1997) showed that starch structural properties are different in root tubers planted and harvested at different dates, and the main reason is the change of environment temperature during root tuber development. dos Santos et al. (2023) investigated the influences of dry and rainy seasons on starch characteristics of sweet potato. The rainy and dry seasons have high and low soil temperatures, respectively, and the rainy season increases the ordered structure and gelatinization temperature of starch, but decreases the hydrolysis of starch (dos Santos et al., 2023). Over 70% production of sweet potato in the world comes from Asian (Alam, 2021). In Asian, sweet potatoes can be planted from April to August, and root tubers are harvested from August to November. The different planting and harvesting dates of sweet potato represent different temperature soils (Noda et al., 1997). However, the effects of natural high temperature (HT) and low temperature (LT) soils on starch characteristics are unclear in sweet potato.

In this study, 3 sweet potato varieties were planted and harvested on July 1 and August 30 in the natural HT field soil and September 1 and October 30 in LT field soil. Our objective is to study the influences of natural field soil temperature on morphology, molecular components, amylopectin branch-chain distribution, crystalline and lamellar structure, thermal properties, and enzyme hydrolysis of starches from sweet potato root tubers. The results would be helpful for breeders, farmers and starch users of sweet potato.

2. Materials and methods

2.1. Materials

Three popular sweet potato varieties Ningzishu 1 (NZS1) with purple-fleshed root tuber, Shushu 16 (SS16) with yellow-fleshed root tuber and Sushu 28 (SS28) with white-fleshed root tuber were planted in the experimental field of Yangzhou University (latitude 32°23′43″ N, longitude 119°25′46″ E, altitude 8 m), Yangzhou, in 2020. They were developed through different parental hybridization and provided by Institute of Food Crops, Jiangsu Academy of Agricultural Sciences, Nanjing, China. Field management and fertilizer treatment were the same among 3 varieties. During sweet potato growth, the daily soil temperature at 10 cm underground was measured at 8:00 and 18:00 (Fig. S1). Two planting and harvesting dates were used in this research. For the first planting and harvesting date, the cuttings were planted on July 1 and root tubers were harvested on August 30, and the root tubers were considered as growth in HT soil due to that the bulking stage of root tuber had soil temperature from about 25 to 30 °C at 8:00 and from about 26 to 32 °C at 18:00. For the second planting and harvesting date, the cuttings were planted on September 1 and root tubers were harvested on October 30, and the root tubers were considered as growth in LT soil due to that the bulking stage of root tuber had soil temperature from about 17 to 23 °C at 8:00 and from about 19 to 23 °C at 18:00 (Fig. S1).

8-Aminopyrene-1,3,6-trisulfonic acid trisodium salt (APTS) (09341), porcine pancreatic α-amylase (PPA) (A3176) and protease from *Streptomyces griseus* (P5147) were purchased from Sigma-Aldrich Chemical Co. (Shanghai, China). Isoamylase (*E*-ISAMY), *Aspergillus niger* amyloglucosidase (AAG) (E-AMGDF), D-glucose Assay Kit (K-GLUC) and Total Starch Assay Kit (K-TSTA) were purchased from Megazyme (Bray, Ireland). All chemicals were analytical grade or better and purchased from Sangon Biotech (Shanghai, China).

2.2. Isolation of starches from root tubers

Starch was isolated following the procedures of Guo et al. (2019). Briefly, fresh root tubers were washed and chopped into small pieces, and then homogenized thoroughly in water using a household kitchen mixer. Sample was filtered through 4 layers of cheesecloth and 100-, 200-, 300-mesh sieves. Starch and water slurry stood for over 5 h. Precipitated starch was washed with water until a clear supernatant. Finally, starch was washed with anhydrous ethanol thrice and dried at 40 °C for 2 d.

2.3. Shape observation and size analysis of starch granules

The shape observation and size analysis of isolated starch followed the methods of Man et al. (2012) with some modifications. Starch in 50% glycerol aqueous solution was detected under a polarized microscope (BX53, Olympus, Japan). Three slides were prepared for every sample, and over 5 regions were randomly chosen and photographed for every slide. Over 2000 starch granules were analyzed for every sample. The areas of starch granules were measured using an Image-Pro Plus 6.0 soft. Starch granules were designated as spherical granules, and their size [d(0.5)] and [D(4,3)] were calculated according to the volume percentages of starch granules.

2.4. Iodine colorimetry analysis of starch

Iodine colorimetry of starch followed the method of Guo et al. (2019). Starch was dispersed into amylopectin and amylose in urea-dimethyl sulfoxide solution at 95 °C. The cooled sample was colored with iodine solution, and scanned from 400 to 900 nm with a spectrophotometer. Apparent amylose content (AAC) was calculated using OD620 with a reference of maize amylopectin and potato amylose.

2.5. Molecular component analysis of starch

Molecular components of starch including amylopectin long branch-chains (AP_L), amylopectin short branch-chains (AP_S) and amylose molecules (AM) were evaluated using gel permeation chromatography (GPC) (PL-GPC 220, Agilent, USA). The detailed starch treatment was the same with that of Lin et al. (2016). The isoamylase-debranched starch sample was analyzed using a high temperature chromatograph with three columns (PL110–6100, 6300, 6525) and a differential refractive index detector. The sample was washed using DMSO containing 0.5 mM $NaNO_3$ at 0.8 mL/min. The column oven temperature was controlled at 80 °C (Cai, Cai, Man, Zhou, & Wei, 2014).

2.6. Branch-chain distribution analysis of amylopectin

The structure of amylopectin was analyzed with a Fluorophore-assisted Capillary Electrophoresis (FACE) system (PA800, Beckman, USA). The detailed sample treatment and testing conditions were the

same with that of Lin et al. (2016). The N-CHO coated capillary (50 μm I. D., 50.2 cm total length) was obtained from Beckman-Coulter. Separations were conducted at 23.5 kV at 25 °C for 80 min.

2.7. Crystalline structure analysis of starch

Starch was detected with an X-ray powder diffractometer (XRD) (D8 Advance, Bruker, Germany). The sample was exposed to the X-ray beam at 200 mA and 40 kV. The scanning region of the diffraction angle (2θ) was from 3° to 40° with a step size of 0.02° and a count time of 0.8 s. Starch treatment and relative crystallinity (RC) measurement were all the same with that of Wei et al. (2010).

2.8. Lamellar structure analysis of starch

Starch-water slurry was analyzed using a small-angle X-ray scattering (SAXS) analysis system (NanoStar, Bruker, Germany) equipped with Vantec 2000 detector and pin-hole collimation for point focus geometry. The X-ray source was a copper rotating anode (0.1 mm filament) operating at 50 kV and 30 W, fitted with cross coupled Göbel mirrors, resulting in Cu Ka radiation wavelength of 1.5418 Å. Starch treatment and lamellar parameter measurement were all the same with the methods of Cai et al. (2014). In order to compare the lamellar peak intensities among different starches, the intensities at scattering vector 0.2 $Å^{-1}$ were all normalized to 20.

2.9. Thermal property analysis of starch

Starch (5 mg) was weighed in aluminum pan, and water (15 μL) was added and sealed. Sample was equilibrated for over 2 h, and then heated with a differential scanning calorimetry (DSC) (200-F3, Netzsch, Germany) at 10 °C/min from 30 to 130 °C. The gelatinization onset temperature (To), peak temperature (Tp), conclusion temperature (Tc) and enthalpy (ΔH) were evaluated from thermogram using the analysis software from DSC manufacturer.

2.10. Enzyme dynamic hydrolysis analysis of starch

Native starch was hydrolyzed by both PPA and AAG at 37 °C completely following the method of Lin et al. (2018). The produced soluble carbohydrates were determined with anthrone-H_2SO_4 method. The degrees of hydrolysis at 10, 20, 40 min and 1, 2, 4, 6, 8, 10, 12, 14, 24 h were modeled using a first-order rate equation $C_t = C_\infty(1–e^{-kt})$, where C_t is the hydrolysis degree of starch at time t, C_∞ is the predicted maximum hydrolysis degree during the hydrolysis, and k is hydrolysis rate constant. The C_∞ and k were fitted using Microsoft Excel Solver by minimizing the sum of squares of residuals (SUMSQ), and the determination coefficient (r^2) and mean relative deviation modulus (MRDM), a predictive ability parameter of the fitted model, were evaluated according to the method of Mahasukhonthachat, Sopade, and Gidley (2010).

2.11. Digestion analysis of starch

Digestions of native and gelatinized starch were investigated completely following the method of Guo et al. (2019). Briefly, starch was hydrolyzed by both PPA and AAG at 37 °C. The produced glucose determined by D-glucose Assay Kit was converted to degraded starch. Total starch was determined with Total Starch Assay Kit. The percentage of degraded starch to total starch within 20 min and between 20 and 120 min was defined as rapidly digestible starch (RDS) and slowly digestible starch (SDS), respectively, and the percentage of residual starch at 120 min hydrolysis was resistant starch (RS).

2.12. Principal component analysis

Minitab 16 was used for principal component analysis (PCA) based on starch characteristics data with the significance of normal distribution over 0.05. The score and loading plots for first 2 components were given.

2.13. Statistical analysis

The analyses of GPC, FACE, XRD and SAXS were repeated two times, and the other experiments were repeated three times. The significance of data normal distribution and the significant difference of data were investigated using Shapiro-Wilk test and Tukey's one-way ANOVA of SPSS 16.0, respectively.

3. Results and discussion

3.1. Granule shape and size of starch

Granule shape and size are important factors affecting functional properties and utilization of starch in food and non-food industries (Li et al., 2022; Lin et al., 2016; Mahasukhonthachat et al., 2010). Isolated starch was observed under polarized microscope (Fig. S2). Under normal light, starch granules exhibited some round, polygonal, oval and semi-oval shapes and had different granule sizes. Under polarized light, starch granules showed central “Maltese crosses”. Starches from root tubers grown in HT and LT soils had no significant differences in granule shapes (Fig. S2). Similar shapes of starch granules have been reported in sweet potato root tuber (dos Santos et al., 2023; Guo et al., 2022). Though the shape of starch granule is attributed to botanical source (Jane, Kasemsuwan, Leas, Zobel, & Robyt, 1994), the growth environment, especially temperature, influences starch size (Emmambux & Taylor, 2013). The granule size analysis exhibited that starch size d(0.5) and D[4,3] among 3 sweet potato varieties ranged from 19.22 to 20.96 μm and from 19.94 to 21.78 μm, respectively, in root tubers grown in HT soil and from 17.77 to 18.15 μm and from 18.03 to 18.69 μm, respectively, in LT soil (Table 1). Noda et al. (2001) reported that sweet potato starch increases granule size when root tuber grows at soil temperature from 15 to 27 °C, but less changes size from 27 to 33 °C. Guo et al. (2022) found that starch granule size increases markedly when soil temperature increases from 21 to 25 °C, but maintains similarly in root tubers grown in 25 and 28 °C soil. In fact, the effect of growth temperature on granule size is also cultivar/species specific, as the granule sizes in some cultivars/species are not changed or even increased/decreased (Li, Daygon, Solah, & Dhital, 2023). Though precise mechanism for determining the size of starch granules is not well understood (Noda et al., 2001), the

Table 1
Granule sizes, blue values and apparent amylose contents of starches from 3 sweet potato varieties grown in HT and LT soils.[a]

	Granule size		BV[b]	AAC (%)[b]
	d(50) (μm)[b]	D[4,3] (μm)[b]		
NZS1-HT	19.22 ± 0.47bc	19.94 ± 0.46b	0.321 ± 0.006c	26.1 ± 0.7c
NZS1-LT	17.77 ± 0.46a	18.03 ± 0.55a	0.256 ± 0.002a	17.8 ± 0.6a
SS16-HT	19.63 ± 0.37c	20.46 ± 0.69b	0.317 ± 0.013c	25.0 ± 1.3c
SS16-LT	18.15 ± 0.51ab	18.69 ± 0.42a	0.290 ± 0.009b	22.5 ± 0.4b
SS28-HT	20.96 ± 0.72d	21.78 ± 0.64c	0.313 ± 0.008c	25.2 ± 0.7c
SS28-LT	17.97 ± 0.30a	18.32 ± 0.22a	0.260 ± 0.009a	18.3 ± 0.3a
Sig.[c]	0.38	0.55	0.135	0.156

[a] Data are means ± standard deviations ($n = 3$). Values in the same column with different letters are significantly different ($p < 0.05$).
[b] d(50), granule size at which 50% of all the granules by volume are smaller; D[4,3], volume-weighted mean diameter; BV, blue value (absorbance of starch-iodine complex at OD680); AAC, apparent amylose content determined by iodine colorimetry and evaluated using OD620.
[c] The significance of normal distribution of these data by Shapiro-Wilk test.

suitable temperature is profit for the development of starch due to that the higher and lower temperature decreases the activity of starch biosynthetic enzymes (Li et al., 2023).

3.2. Iodine absorption and AAC of starch

Iodine absorption spectrum of starch can reflect the contents of amylose and amylopectin due to their having different iodine affinity abilities (Lin, Zhang, Zhang, & Wei, 2017). Starches from root tubers grown in HT soil all exhibited stronger iodine absorption than those in LT soil among 3 sweet potato varieties according to their iodine absorption spectra (Fig. S3). The blue value (BV), the absorbance of starch-iodine complex at OD680, is usually used to reflect the binding ability of starch and iodine. The 3 starches from root tubers grown in HT and LT soils had BV from 0.313 to 0.321 and from 0.256 to 0.290, respectively (Table 1), indicating that HT soil could significantly induce the increase of the iodine affinity of starch. The amylose content of starch determined using iodine colorimetry method is defined usually as AAC due to that the amylopectin branch-chains also bind iodine and AAC contains partial amylopectin (Lin et al., 2017). The AACs of starches from root tubers grown in HT and LT soils were 26.1% and 17.8% for NZS1, 25.0% and 22.5% for SS16 and 25.2% and 18.3% for SS28, respectively (Table 1), indicating that HT soil significantly induced the increase of the AAC. The effects of growth temperature on iodine absorption and AAC of starch have been reported during root tuber development of sweet potato. Noda et al. (1997) reported that though sweet potato root tubers with different planting and harvesting dates are subjected to different temperature soils in the field, they have no significant relationship with AAC of starch determined by BV. However, Noda et al. (2001) reported that AAC determined by BV increases significantly in sweet potato cultivar Ayamurasaki and Sunnyred with increasing soil temperature controlled by a greenhouse from 15 to 33 °C. The discrepancy might result from different cultivars, measuring methods and plant planting ways.

3.3. Molecular component contents of starch

The molecular weight distribution of starch is usually analyzed using GPC, and can be used to accurately evaluate the molecular component contents of starch (Fan et al., 2020). In the present study, molecular weight distributions of starches are analyzed using GPC (Fig. S4). The peak 1, 2 and 3 in GPC profile of isoamylase-debranched starch represent AP_S, AP_L and AM, respectively, according to their molecular weights from low to high. Their area percentages are usually defined as their content percentage, and the content ratio of AP_S to AP_L (AP_S/AP_L) is usually used as an index of branching degree of amylopectin (Lin et al., 2017). In this research, starches from root tubers grown in HT and LT soils had similar amylose contents among 3 sweet potato varieties, but their AP_S contents and AP_S/AP_L in root tuber grown in HT soil were lower and AP_L contents were higher than those in LT soil (Table 2), indicating that HT soil could induce the increase of the branch-chain length of amylopectin. Guo et al. (2022) also reported that growth temperature does not change amylose content of starch when sweet potato is planted in constant-temperature chambers, but high growth temperature decreases the AP_S and increase the AP_L. Zhu, Yang, Cai, Bertoft, and Corke (2011) found that amylose contents of 11 sweet potato starches range from 23.3% to 26.5% by iodine colorimetry, from 17.5% to 23.9% by GPC and from 15.9% to 22.5% by concanavalin A precipitation. The high amylose content by iodine colorimetry is attributed to iodine binding by AP_L. Amylose is synthesized by granule-bound starch synthase I (GBSSI) (Huang, Sreenivasulu, & Liu, 2020). The expression level of GBSSI gene (*Waxy*) does not significantly change in sweet potato root tuber grown at different temperatures (Guo et al., 2022), agreeing with the present results (Table 2).

Table 2
Molecular components of starches from 3 sweet potato varieties grown in HT and LT soils.[a]

	AP_S (%)[b]	AP_L (%)[b]	AM (%)[b]	AP_S/AP_L
NZS1-HT	57.7 ± 0.5abc	24.0 ± 0.3bc	18.8 ± 0.0ab	2.40 ± 0.01ab
NZS1-LT	59.2 ± 1.7bcd	22.6 ± 1.3b	18.3 ± 0.3a	2.63 ± 0.23bc
SS16-HT	57.0 ± 0.3ab	22.8 ± 0.3b	20.3 ± 0.0b	2.50 ± 0.04ab
SS16-LT	61.9 ± 1.0d	19.2 ± 0.3a	18.9 ± 0.7ab	3.22 ± 0.10d
SS28-HT	55.7 ± 0.5a	25.2 ± 0.3c	19.2 ± 0.2ab	2.21 ± 0.04a
SS28-LT	60.5 ± 0.2cd	20.4 ± 0.2a	19.1 ± 0.4ab	2.96 ± 0.03cd
Sig.[c]	0.927	0.837	0.309	0.783

[a] Data are means ± standard deviations ($n = 2$). Values in the same column with different letters are significantly different ($p < 0.05$).
[b] AP_S, amylopectin short branch-chains; AP_L, amylopectin long branch-chains; AM, amylose molecules; AP_S/AP_L, content ratio of AP_S to AP_L.
[c] The significance of normal distribution of these data by Shapiro-Wilk test.

3.4. Branch-chain distribution of amylopectin

In order to further reveal the amylopectin change in root tubers grown in HT and LT soils, isoamylase-debranched amylopectin was analyzed using FACE (Fig. S5). The branch-chains with DP6–16 in root tuber grown in HT soil were lower and those with DP ≥ 18 were higher than those in LT soil for 3 sweet potato varieties. The branch-chains of amylopectin were usually classified into A, B1, B2 and B3+ branch-chains with DP6–12, DP13–24, DP25–36 and DP ≥ 37, respectively (Guo et al., 2022; Wei et al., 2010). Compared with amylopectin in root tuber grown in HT soil, amylopectin in root tuber grown in LT soil increased A branch-chains and decreased B2 and B3+ branch-chains, leading to a significant decrease of average branch-chain length (ACL) (Table 3). In general, amylopectin structure is sensitive to growth temperatures. High growth temperature can decrease amylopectin A branch-chains and increase B2 and B3+ branch-chains in sweet potato root tuber (Guo et al., 2022; Noda et al., 2001). Similar results about the effects of growth temperature on amylopectin structure are also reported in potato (Orawetz, Malinova, Orzechowski, & Fettke, 2016) and cereal crops (Fan et al., 2020; Yang et al., 2021). Amylopectin is synthesized by soluble starch synthases (SSs) for extending amylopectin branch-chains, starch branching enzymes (SBEs) for producing new branch-chains, and starch debranching enzymes for removing some branch-chains (Huang, Tan, Zhang, Li, & Liu, 2021). Guo et al. (2022) analyzed the expression of starch biosynthesis-related genes in sweet potato root tuber grown in chambers with different growth temperatures, and found that HT soil increases the expressions of isoamylase1, SSIII and SBEI genes, responsible for producing less amylopectin A branch-chains and increases the contents of B2 and B3+ branch-chains. Therefore, the HT soil during sweet potato root tuber growth could extend amylopectin branch-chains, leading to the increase of iodine affinity and AAC of starch (Table 1).

3.5. Crystalline structure of starch

Branch-chain double helices of amylopectin can form A-type or B-type crystallinity due to their different arrangement patterns. Starches from different plant resources are usually divided into A-type with only A-type crystallinity, B-type with only B-type crystallinity and C-type with both A- and B-type crystallinity according to their XRD patterns. C-type starches can be further divided into C_A-, C_C- and C_B-type according to their XRD patterns produced by the content ratio of A- and B-type crystallinity from high to low (He & Wei, 2017). Starches from root tubers grown in LT soil exhibited C_C-type XRD patterns with strong diffraction peak at 2θ 17° and weak peaks at 2θ 23°, 15° and 5.6° among 3 sweet potato varieties. However, starches from root tubers grown in HT soil had very similar A-type XRD patterns with significant doublet at 2θ 17° and 18° and strong diffraction peaks at 2θ 15° and 23°, but the very weak peak at 2θ 5.6°, a characteristic peak of B-type crystallinity, could also be detected, indicating that they contained a small amount of

Table 3
Branch-chain length distributions of amylopectins, relative crystallinities and lamellar structural parameters of starches from 3 sweet potato varieties grown in HT and LT soils.[a]

	Branch-chain length distribution of amylopectin					RC (%)[b]	PI (counts)[b]	D (nm)[b]
	DP6–12 (%)	DP13–24 (%)	DP25–36 (%)	DP ≥ 37 (%)	ACL (DP)[b]			
NZS1-HT	19.1 ± 0.1a	46.8 ± 0.0c	15.3 ± 0.0c	18.8 ± 0.2b	24.7 ± 0.1c	29.7 ± 0.6d	432.0 ± 46.3c	10.04 ± 0.01b
NZS1-LT	22.9 ± 0.1c	46.6 ± 0.2c	13.7 ± 0.0a	16.8 ± 0.1b	23.1 ± 0.1b	24.7 ± 0.3b	239.2 ± 14.3ab	9.76 ± 0.01a
SS16-HT	19.1 ± 0.1a	47.4 ± 0.0c	15.9 ± 0.1d	17.6 ± 0.2b	24.1 ± 0.1c	27.5 ± 0.2c	411.8 ± 17.4c	10.27 ± 0.03d
SS16-LT	24.0 ± 0.1d	47.2 ± 0.2c	14.5 ± 0.1b	14.2 ± 0.2a	22.0 ± 0.1a	25.1 ± 0.3bc	260.5 ± 11.4b	10.30 ± 0.01d
SS28-HT	21.4 ± 0.3b	44.6 ± 0.7b	15.2 ± 0.3c	18.8 ± 1.3b	24.4 ± 0.6c	26.7 ± 0.6bc	366.8 ± 2.8c	10.21 ± 0.02c
SS28-LT	27.7 ± 0.0e	43.6 ± 0.1a	14.0 ± 0.0a	14.7 ± 0.1a	21.9 ± 0.1a	21.2 ± 1.3a	176.2 ± 1.4a	10.31 ± 0.01d
Sig.[c]	0.546	0.131	0.819	0.291	0.266	0.953	0.505	0.069

[a] Data are means ± standard deviations ($n = 2$). Values in the same column with different letters are significantly different ($p < 0.05$).
[b] ACL, average Branch-chain length; DP, degree of polymerization; RC, relative crystallinity; PI, lamellar peak intensity; D, lamellar repeat distance.
[c] The significance of normal distribution of these data by Shapiro-Wilk test.

B-type crystallinity and were C_A-type starches (Fig. 1). A-, C_A-, C_C-, C_B-type XRD patterns are all reported in starches from sweet potato root tubers. The complicated crystalline polymorphic structure is due to the fact that the crystalline structure formation is sensitive to growth conditions of root tuber, especially soil temperature (dos Santos et al., 2023; Genkina et al., 2003; Genkina, Wasserman, Noda, Tester, & Yuryev, 2004; Guo et al., 2022). Genkina et al. (2003, 2004) detected that sweet potatoes have A-type starches in root tubers grown in 27 and 33 °C soil, gradually form and accumulate B-type crystallinity with decreasing soil temperature, and have C_B-type starch in root tubers grown in 15 °C soil. Guo et al. (2022) detected that sweet potato starch exhibits C_C-type, C_A-type and closest to A-type XRD pattern in root tuber grown in 21, 25 and 28 °C soil, respectively. dos Santos et al. (2023) detected that sweet potato starch shows A-type XRD pattern in root tuber grown in rainy season with high soil temperature and C_A-type in dry season with low soil temperature. Though the short and long branch-chains of amylopectin are prone to form A- and B-type starch at the same condition, respectively, B-type crystallinity forms under cool and wet conditions and A-type crystallinity forms in warm and dry conditions. In addition, the B-type crystallinity can irreversibly transit to A-type under conditions of low humidity and HT through rearrangement of the pairs of double helices (Pérez et al., 2009). In this research, sweet potato had C_A-type starch with increased AP_L in root tubers grown in HT soil and C_C-type starch with increased AP_S in root tubers grown in LT soil (Fig. 1, Table 2), indicating that the soil temperature might play more important role in crystallinity formation than the amylopectin branch-chain length in sweet potato. The RC of sweet potato starch from root tuber grown in HT soil was significantly higher than that in LT soil (Table 3), agreeing with the recent report (Guo et al., 2022). Usually, RC has positive relationship with amylopectin content. In the present study, the amylopectin contents are similar in starches from root tubers grown in HT and LT soils, but their branch-chain distributions are different. Zhong et al. (2021) reported that the B2 and B3+ branch-chains of amylopectin can improve the crystalline ordering, agreeing with the present results.

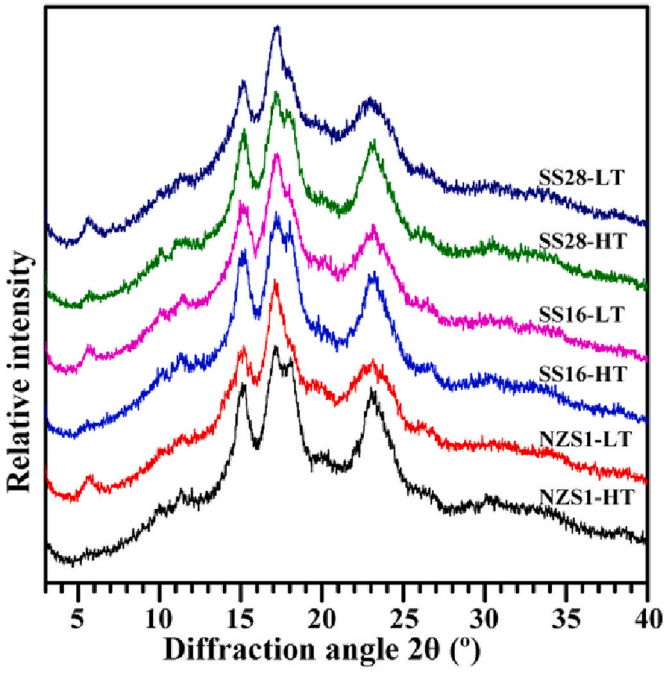

Fig. 1. XRD patterns of starches from 3 sweet potato varieties grown in HT and LT soils.

3.6. Lamellar structure of starch

Starch lamellar structure is important controller of physicochemical, gelatinization and digestion properties, and can be analyzed with SAXS (Li & Gong, 2021; Xu, Blennow, Li, Chen, & Liu, 2020). The SAXS profiles of starches were presented in Fig. S6, and their peak intensity (PI) and lamellar repeat distance (D) were presented in Table 3. Though starches from root tubers grown in HT and LT soils had similar lamellar repeat distances, their lamellar peak intensities were significantly higher in HT soil than those in LT soil (Table 3). The PI reflects electron density differences between crystalline and amorphous lamellae (Yuryev et al., 2004), and can quantify the ordered degree of starch semicrystalline structure (Blazek & Gilbert, 2011). Usually, lamellar PI has positive relationship with RC and AP_L (Cai et al., 2015; Zhong et al., 2021). In this research, high lamellar PI of starch from root tuber grown in HT soil agreed with its high RC and increased AP_L (Table 3).

3.7. Thermal properties of starch

Thermal properties of starch play important roles in food processing, and can be measured using DSC (Li et al., 2022; Xu et al., 2020). The DSC thermograms showed significant differences between starches from root tubers grown in HT and LT soils (Fig. S7). Starches from root tubers grown in HT soil had significantly higher gelatinization temperature with To from 65.5 to 71.5 °C, Tp from 72.0 to 76.8 °C and Tc from 78.9 to 82.7 °C than those in LT soil with To from 51.1 to 55.3 °C, Tp from 56.4 to 63.4 °C and Tc from 67.6 to 72.4 °C among 3 sweet potato varieties. Gelatinization temperature ranges (ΔT) of starches from root tubers grown in LT soil were wider than those in HT soil (Table 4). Similar phenomena are detected in sweet potato grown in controlled environment growth chamber at different temperatures (Guo et al., 2022). The HT soil significantly induced the increase of starch gelatinization temperature in sweet potato (Noda et al., 2001). Many references reported that sweet potato starches have very wide ΔT when root tubers grow in soil containing a wide range of temperature (Genkina et al., 2004; Guo, Zhang, Bian, Cao, & Wei, 2020; Li et al., 2022). Guo

Table 4
Thermal property parameters of starches from 3 sweet potato varieties grown in HT and LT soils.[a]

	To (°C) [b]	Tp (°C)[b]	Tc (°C)[b]	ΔT (°C)[b]	ΔH (J/g)[b]
NZS1-HT	71.5 ± 0.0f	76.8 ± 0.1f	82.7 ± 0.3e	11.2 ± 0.3a	11.1 ± 0.8bc
NZS1-LT	55.3 ± 0.3c	61.2 ± 0.9b	71.8 ± 0.2b	16.5 ± 0.3c	10.6 ± 0.4abc
SS16-HT	70.3 ± 0.3e	74.9 ± 0.2e	81.3 ± 0.1d	11.0 ± 0.4a	12.0 ± 1.3c
SS16-LT	54.6 ± 0.3b	63.4 ± 0.3c	72.4 ± 0.6b	17.8 ± 0.4d	9.4 ± 0.3ab
SS28-HT	65.5 ± 0.1d	72.0 ± 0.2d	78.9 ± 0.3c	13.4 ± 0.3b	10.0 ± 0.7ab
SS28-LT	51.1 ± 0.1a	56.4 ± 0.7a	67.6 ± 0.7a	16.4 ± 0.7c	8.9 ± 0.2a
Sig.[c]	0.248	0.512	0.498	0.246	0.967

[a] Data are means ± standard deviations ($n = 3$). Values in the same column with different letters are significantly different ($p < 0.05$).
[b] To, gelatinization onset temperature; Tp, gelatinization peak temperature; Tc, gelatinization conclusion temperature; ΔT, gelatinization temperature range (Tc - To); ΔH, gelatinization enthalpy.
[c] The significance of normal distribution of these data by Shapiro-Wilk test.

et al. (2020) reported that root tuber of sweet potato simultaneously has A-type starch granules with high gelatinization temperature, B-type starch granules with low gelatinization temperature and C-type starch granules with intermediate gelatinization temperature, resulting in a very wide DSC thermal peak. Amylose content and amylopectin structure take crucial roles in starch gelatinization. Gelatinization temperature has negative relationship with content of amylopectin branch-chains with DP6–12 (Cai et al., 2015; Zhang et al., 2020). In this research, though starches from root tubers grown in HT and LT soils exhibited different apparent amylose contents (Table 1), they had similar amylose contents (Table 2). The high gelatinization temperature of starch from root tuber grown in HT soil might be attributed to low content of amylopectin branch-chains with DP6–12 (Table 3).

3.8. Enzyme dynamic hydrolysis of starch

The enzyme hydrolysis of starch is a dynamic process (Lin et al., 2018). The dynamic hydrolysis degrees of native starch by both PPA and AMG were fitted following first-order rate equation (Fig. S8). The fitted hydrolysis profiles and their parameters indicated the suitability of the procedure (SUMSQ <88.8, MRDM <12.4, $r^2 > 0.994$) (Table 5). Though the hydrolysis extents showed some differences among starches from 3 varieties, their hydrolysis rate coefficients ranged from 0.120 to 0.163 h^{-1} in HT soil and from 0.227 to 0.282 h^{-1} in LT soil, indicating that starches from root tubers grown in LT soil were hydrolyzed significantly more rapidly than those in HT soil (Table 5). Noda et al. (2001) reported that the hydrolysis rate of starch decreases with increase of soil temperature from 15 to 33 °C in sweet potato. For native starch, the hydrolysis rate is significantly correlated positively to AP_S content, and negatively to granule size and contents of amylose content and AP_L (Cai et al., 2015; Lin et al., 2016). Therefore, high resistance of sweet potato starch from root tuber grown in HT soil to enzyme hydrolysis might result from large granule size and high AP_L content (Table 1, Table 2).

Table 5
Dynamic hydrolysis parameters of starches from 3 sweet potato varieties grown in HT and LT soils.[a]

	C∞ (%)[b]	k (h^{-1})[b]	SUMSQ[b]	MRDM (%)[b]	r^2[b]
NZS1-HT	95.1 ± 0.9bc	0.120 ± 0.009a	< 33.0	< 11.1	> 0.997
NZS1-LT	93.8 ± 0.3b	0.227 ± 0.026b	< 23.8	< 10.0	> 0.998
SS16-HT	97.5 ± 1.0c	0.163 ± 0.006a	< 88.8	< 6.4	> 0.994
SS16-LT	94.1 ± 0.8b	0.227 ± 0.006b	< 35.6	< 8.2	> 0.998
SS28-HT	90.5 ± 1.2a	0.156 ± 0.007a	< 47.2	< 12.4	> 0.997
SS28-LT	95.4 ± 0.1bc	0.282 ± 0.008c	< 10.5	< 4.5	> 0.999
Sig.[c]	0.763	0.711	–	–	–

[a] Data are means ± standard deviations ($n = 3$). Values in the same column with different letters are significantly different ($p < 0.05$).
[b] C∞, starch hydrolysis extent; k, hydrolysis rate coefficient; SUMSQ, sum of squares of residuals; MRDM, mean relative deviation modulus; r^2, determination coefficient.
[c] The significance of normal distribution of these data by Shapiro-Wilk test.

3.9. Digestion of starch

The *in vitro* digestion of starch by both PPA and AAG is usually employed to simulate the effects of small intestine hydrolysis and subsequent glycemic response of starch, and can provide some information for the applications of starch in food industry (Englyst, Kingman, & Cummings, 1992). The glucose released from native and gelatinized starch by both PPA and AMG was measured (Table 6). The 3 native starches from root tubers grown in HT soil had RDS from 3.1% to 5.4%, SDS from 12.8% to 18.4%, and RS from 76.2% to 84.1%, and those in LT soil had RDS from 5.2% to 8.9%, SDS from 20.9% to 31.8%, and RS from 59.2% to 72.8%, indicating that HT soil could induce the decrease of RDS and SDS and the increase of RS. Native starch is semicrystalline granule structure, and has differences in shape, size and crystalline structure (Emmambux & Taylor, 2013; He & Wei, 2017; Pérez et al., 2009). The small granule starch is digested more rapidly than large granule. The contents of amylose and AP_L have negative relationships with starch digestion, but AP_S have a positive relationship with starch digestion (Lin et al., 2016). Usually, A-type crystallinity is degraded more rapidly than B-type crystallinity, but the starch from root tuber grown in HT soil contained more A-type crystallinity than B-type crystallinity. Therefore, starch size and amylopectin branch-chains took main roles in determining native starch digestion in the present research. The gelatinized starch from root tubers grown in HT and LT soils had similar RDS, SDS and RS (Table 6). Granule swells and crystallinity is disrupted during starch gelatinization, and starch components play important roles in starch digestion (Guo et al., 2019). Though starches from root tubers grown in HT and LT soils had similar amylose

Table 6
Digestion properties of starches from 3 sweet potato varieties grown in HT and LT soils.[a]

	Native starch digestion			Gelatinized starch digestion		
	N-RDS (%)[b]	N-SDS (%)[b]	N-RS (%)[b]	G-RDS (%)[b]	G-SDS (%)[b]	G-RS (%)[b]
NZS1-HT	3.1 ± 0.3a	12.8 ± 0.2a	84.1 ± 0.2f	77.6 ± 0.7a	2.7 ± 0.3a	19.7 ± 0.8a
NZS1-LT	5.2 ± 0.4bc	25.4 ± 0.2e	69.4 ± 0.5b	78.7 ± 0.9a	2.5 ± 0.1a	18.8 ± 0.9a
SS16-HT	4.1 ± 0.4ab	16.0 ± 0.7b	79.9 ± 1.1e	77.9 ± 1.1a	4.7 ± 0.4b	17.3 ± 0.8a
SS16-LT	6.3 ± 0.5c	20.9 ± 0.8d	72.8 ± 0.9c	77.5 ± 1.0a	4.4 ± 0.8b	18.1 ± 1.3a
SS28-HT	5.4 ± 0.6bc	18.4 ± 0.3c	76.2 ± 0.4d	77.2 ± 0.4a	2.8 ± 0.7a	19.9 ± 1.0a
SS28-LT	8.9 ± 0.8d	31.8 ± 0.4f	59.2 ± 0.6a	78.6 ± 1.2a	3.8 ± 0.5ab	17.6 ± 0.7a
Sig.[c]	0.744	0.87	0.893	0.293	0.284	0.422

[a] Data are means ± standard deviations ($n = 3$). Values in the same column with different letters are significantly different ($p < 0.05$).
[b] RDS, rapidly digestible starch; SDS, slowly digestible starch; RS, resistant starch; N-, native starch; G-, gelatinized starch.
[c] The significance of normal distribution of these data by Shapiro-Wilk test.

contents, their amylopectin branch-chains were significantly different, indicating that the branch-chains of amylopectin might have less effect on digestion of gelatinized starch.

3.10. PCA of starch

In order to further reveal the relationships of property parameters of starches from root tubers grown in HT and LT soil, we carried out the PCA based on the above property parameter data (Fig. 2). The principal component 1 and 2 could clarify 65.8% and 16.7% of total variance, respectively. Relationships among different physicochemical properties can be detected using loading plot of PCA. For starch components, the branch-chain with DP6–12 was highly negatively correlated to BV, and branch-chain with DP25–36 was highly positively correlated to BV and AAC. For starch component and crystalline structure, the lamellar PI and RC were highly positively correlated ($p < 0.01$), and they were positively correlated to BV, AAC and ACL and negatively correlated to branch-chain with DP6–12. For thermal properties, the gelatinization temperatures (To, Tp, Tc) had highly positive relationships with BV, AAC, AP_L, RC and PI, and negative relationships with AP_S. For starch hydrolysis, the hydrolysis rate coefficient (k) was correlated positively to branch-chains with DP6–12 and negatively to BV, AAC, branch-chains with DP $\geq$ 37, ACL, RC, PI and gelatinization temperature. For native starch digestion, RDS and SDS were positively correlated to branch-chains with DP6–12, and negatively to ACL, RC, PI and gelatinization temperature, but the RS of native starch showed an opposite correlation with the above properties. In addition, starch size had positive correlations with gelatinization temperature and resistant starch of native starch and negative correlation with hydrolysis rate of native starch (Fig. 2A). Based on physicochemical properties of starch, 6 starches were distributed dispersedly in the score plot of PCA. Starches from root tubers grown in HT and LT soils were distributed at the right and left of plot, respectively, implying that soil temperature significantly influenced the physicochemical properties and utilization of sweet potato starch.

4. Conclusions

Starches from root tubers grown in natural HT and LT field soils had significantly different physicochemical characteristics, regardless of their sources of root tuber colors and varieties. Starches from root tuber grown in HT soil had larger granule size and longer amylopectin branch-chains than those in LT soil, but maintained similar granule shape and amylose content between in HT and LT soil. Starches from root tubers grown in HT and LT soils both exhibited C-type XRD patterns, but HT

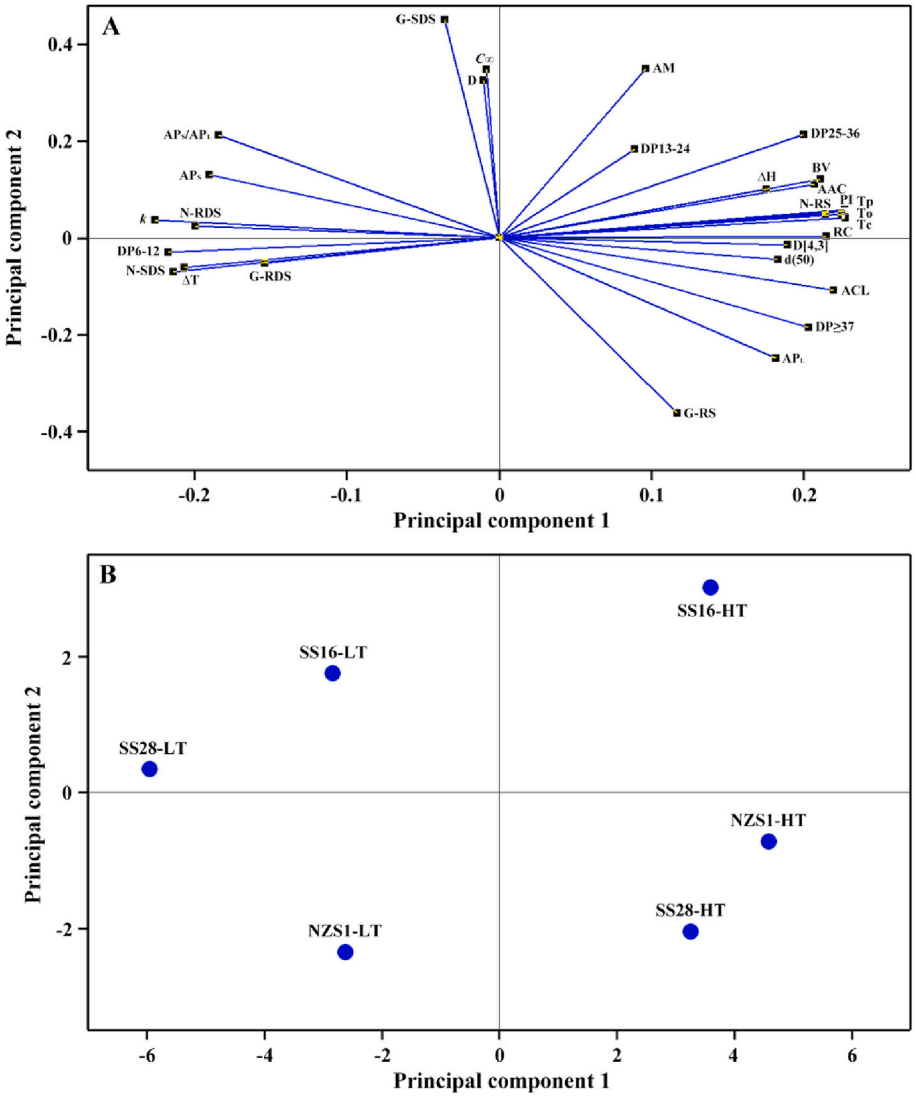

Fig. 2. PCA of physicochemical properties of starches from 3 sweet potato varieties grown in HT and LT soils. (A), loading plot of PCA of starch property parameters; (B), score plot of PCA of starches from 3 sweet potato varieties grown in HT and LT soils.

soil induced the increase of A-type allomorph content, RC and lamellar PI. Starch from root tuber grown in HT soil significantly increased gelatinization temperature and decreased enzyme hydrolysis rate. The differences in granule size, amylopectin structure, semicrystalline structure, thermal properties and enzyme hydrolysis resulted in different potential utilizations of sweet potato starches from root tubers grown in HT and LT soils. The above results could provide evidence that starch properties of sweet potato could be regulated through manipulating planting and/or harvesting dates, and helpful to design planting strategies of sweet potato in order to meet its different applications in food and nonfood industries.

CRediT authorship contribution statement

Laiquan Shi: Writing – original draft, Visualization, Validation, Software, Methodology, Investigation, Formal analysis, Data curation. **Ke Guo:** Visualization, Validation, Software, Methodology, Investigation, Formal analysis, Data curation. **Xin Xu:** Methodology, Data curation. **Lingshang Lin:** Data curation, Methodology. **Xiaofeng Bian:** Resources, Supervision. **Cunxu Wei:** Writing – review & editing, Visualization, Supervision, Project administration, Funding acquisition, Formal analysis, Conceptualization.

Declaration of competing interest

The authors declare that they have no known competing financial interests or personal relationships that could have appeared to influence the work reported in this paper.

Data availability

Data will be made available on request.

Acknowledgement

This work was financially supported by grants from the Priority Academic Program Development of Jiangsu Higher Education Institutions.

Appendix A. Supplementary data

The following Figures were supplied in the Supplementary data, including, Fig. S1: Soil temperatures during sweet potato growth; Fig. S2: Granule shapes of starches from 3 sweet potato varieties grown in HT and LT soils; Fig. S3: The iodine absorption spectra of starches from 3 sweet potato varieties grown in HT and LT soils; Fig. S4: The GPC profiles of isoamylase-debranched starches from 3 sweet potato varieties grown in HT and LT soils; Fig. S5: The branch-chain length distributions of amylopectins from 3 sweet potato varieties grown in HT and LT soils; Fig. S6: SAXS profiles of starches from 3 sweet potato varieties grown in HT and LT soils; Fig. S7: DSC thermograms of starches from 3 sweet potato varieties grown in HT and LT soils; Fig. S8: Experimental hydrolysis degrees, fitted hydrolysis curve, and residuals between experimental and fitted hydrolysis degrees of starches from 3 sweet potato varieties grown in HT and LT soils. Supplementary data to this article can be found online at https://doi.org/10.1016/j.fochx.2024.101346.

References

Alam, M. K. (2021). A comprehensive review of sweet potato (*Ipomoea batatas* [L.] lam): Revisiting the associated health benefits. *Trends in Food Science & Technology, 115*, 512–529. https://doi.org/10.1016/j.tifs.2021.07.001

Blazek, J., & Gilbert, E. P. (2011). Application of small-angle X-ray and neutron scattering techniques to the characterisation of starch structure: A review. *Carbohydrate Polymers, 85*, 281–293. https://doi.org/10.1016/j.carbpol.2011.02.041

Cai, C., Cai, J., Man, J., Yang, Y., Wang, Z., & Wei, C. (2014). Allomorph distribution and granule structure of lotus rhizome C-type starch during gelatinization. *Food Chemistry, 142*, 408–415. https://doi.org/10.1016/j.foodchem.2013.07.091

Cai, J., Cai, C., Man, J., Zhou, W., & Wei, C. (2014). Structural and functional properties of C-type starches. *Carbohydrate Polymers, 101*, 289–300. https://doi.org/10.1016/j.carbpol.2013.09.058

Cai, J., Man, J., Huang, J., Liu, Q., Wei, W., & Wei, C. (2015). Relationship between structure and functional properties of normal rice starches with different amylose contents. *Carbohydrate Polymers, 125*, 35–44. https://doi.org/10.1016/j.carbpol.2015.02.067

Emmambux, M. N., & Taylor, J. R. N. (2013). Morphology, physical, chemical, and functional properties of starches from cereals, legumes, and tubers cultivated in Africa: A review. *Starch, 65*, 715–729. https://doi.org/10.1002/star.201200263

Englyst, H. N., Kingman, S. M., & Cummings, J. H. (1992). Classification and measurement of nutritionally important starch fractions. *European Journal of Clinical Nutrition, 45*, S33–S50.

Fan, X., Li, Y., Zhu, Y., Wang, J., Zhao, J., Sun, X., Pan, Y., Bian, X., Zhang, C., Zhao, D., & Liu, Q. (2020). Characterization of physicochemical qualities and starch structures of two indica rice varieties tolerant to high temperature during grain filling. *Journal of Cereal Science, 93*, Article 102966. https://doi.org/10.1016/j.jcs.2020.102966

Genkina, N. K., Noda, T., Koltisheva, G. I., Wasserman, L. A., Tester, R. F., & Yuryev, V. P. (2003). Effects of growth temperature on some structural properties of crystalline lamellae in starches extracted from sweet potatoes (*Sunnyred* and *Ayamurasaki*). *Starch, 55*, 350–357. https://doi.org/10.1002/star.200300145

Genkina, N. K., Wasserman, L. A., Noda, T., Tester, R. F., & Yuryev, V. P. (2004). Effects of annealing on the polymorphic structure of starches from sweet potatoes (*Ayamurasaki* and *Sunnyred* cultivars) grown at various soil temperatures. *Carbohydrate Research, 339*, 1093–1098. https://doi.org/10.1016/j.carres.2004.01.009

Guo, K., Lin, L., Li, E., Zhong, Y., Petersen, B. L., Blennow, A., … Wei, C. (2022). Effects of growth temperature on multi-scale structure of root tuber starch in sweet potato. *Carbohydrate Polymers, 298*, Article 120136. https://doi.org/10.1016/j.carbpol.2022.120136

Guo, K., Liu, T., Xu, A., Zhang, L., Bian, X., & Wei, C. (2019). Structural and functional properties of starches from root tubers of white, yellow, and purple sweet potatoes. *Food Hydrocolloids, 89*, 829–836. https://doi.org/10.1016/j.foodhyd.2018.11.058

Guo, K., Zhang, L., Bian, X., Cao, Q., & Wei, C. (2020). A-, B-and C-type starch granules coexist in root tuber of sweet potato. *Food Hydrocolloids, 98*, Article 105279. https://doi.org/10.1016/j.foodhyd.2019.105279

He, W., & Wei, C. (2017). Progress in C-type starches from different plant sources. *Food Hydrocolloids, 73*, 162–175. https://doi.org/10.1016/j.foodhyd.2017.07.003

Huang, L., Sreenivasulu, N., & Liu, O. (2020). *Waxy* editing: Old meets new. *Trends in Plant Science, 25*, 963–966. https://doi.org/10.1016/j.tplants.2020.07.009

Huang, L., Tan, H., Zhang, C., Li, Q., & Liu, Q. (2021). Starch biosynthesis in cereal endosperms: An updated review over the last decade. *Plant Communications, 2*, Article 100237. https://doi.org/10.1016/j.xplc.2021.100237

Jane, J. L., Kasemsuwan, T., Leas, S., Zobel, H., & Robyt, J. F. (1994). Anthology of starch granule morphology by scanning electron microscopy. *Starch, 46*, 121–129. https://doi.org/10.1002/star.19940460402

Li, C., & Gong, B. (2021). Relations between rice starch fine molecular and lamellar/crystalline structures. *Food Chemistry, 353*, Article 129467. https://doi.org/10.1016/j.foodchem.2021.129467

Li, M., Daygon, V. D., Solah, V., & Dhital, S. (2023). Starch granule size: Does it matter? *Critical Reviews in Food Science and Nutrition, 63*, 3683–3703. https://doi.org/10.1080/10408398.2021.1992607

Li, Y., Zhao, L., Shi, L., Lin, L., Cao, Q., & Wei, C. (2022). Sizes, components, crystalline structure, and thermal properties of starches from sweet potato varieties originating from different countries. *Molecules, 27*, 1905. https://doi.org/10.3390/molecules27061905

Lin, L., Cai, C., Gilbert, R. G., Li, E., Wang, J., & Wei, C. (2016). Relationships between amylopectin molecular structures and functional properties of different-sized fractions of normal and high-amylose maize starches. *Food Hydrocolloids, 52*, 359–368. https://doi.org/10.1016/j.foodhyd.2015.07.019

Lin, L., Zhang, L., Cai, X., Liu, Q., Zhang, C., & Wei, C. (2018). The relationship between enzyme hydrolysis and the components of rice starches with the same genetic background and amylopectin structure but different amylose contents. *Food Hydrocolloids, 84*, 406–413. https://doi.org/10.1016/j.foodhyd.2018.06.029

Lin, L., Zhang, Q., Zhang, L., & Wei, C. (2017). Evaluation of the molecular structural parameters of normal rice starch and their relationships with its thermal and digestion properties. *Molecules, 22*, 1526. https://doi.org/10.3390/molecules22091526

Mahasukhonthachat, K., Sopade, P. A., & Gidley, M. J. (2010). Kinetics of starch digestion in sorghum as affected by particle size. *Journal of Food Engineering, 96*, 18–28. https://doi.org/10.1016/j.jfoodeng.2009.06.051

Man, J., Cai, J., Cai, C., Xu, B., Huai, H., & Wei, C. (2012). Comparison of physicochemical properties of starches from seed and rhizome of lotus. *Carbohydrate Polymers, 88*, 676–683. https://doi.org/10.1016/j.carbpol.2012.01.016

Noda, T., Kobayashi, T., & Suda, I. (2001). Effect of soil temperature on starch properties of sweet potatoes. *Carbohydrate Polymers, 44*, 239–246. https://doi.org/10.1016/S0144-8617(00)00227-7

Noda, T., Takahata, Y., Sato, T., Ikoma, H., & Mochida, H. (1997). Combined effects of planting and harvesting dates on starch properties of sweet potato roots. *Carbohydrate Polymers, 33*, 169–176. https://doi.org/10.1016/S0144-8617(97)00047-7

Orawetz, T., Malinova, I., Orzechowski, S., & Fettke, J. (2016). Reduction of the plastidial phosphorylase in potato (*Solanum tuberosum* L.) reveals impact on storage

starch structure during growth at low temperature. *Plant Physiology and Biochemistry, 100*, 141–149. https://doi.org/10.1016/j.plaphy.2016.01.013

Pérez, S., Baldwin, P. M., & Gallant, D. J. (2009). Structural features of starch granules I. In J. BeMiller, & R. Whistler (Eds.), *Starch: Chemistry and technology* (3rd ed., pp. 149–192). Elsevier Inc.. https://doi.org/10.1016/B978-0-12-746275-2.00005-7

dos Santos, T. P. R., Leonel, M., de Oliveira, L. A., Fernandes, A. M., Leonel, S., & da Silva Nunes, J. G. (2023). Seasonal variations in the starch properties of sweet potato cultivars. *Horticulturae, 9*, 303. https://doi.org/10.3390/horticulturae9030303

Song, H. G., Choi, I., Lee, J. S., Chung, M. N., Yoon, C. S., & Han, J. (2021). Comparative study on physicochemical properties of starch films prepared from five sweet potato (*Ipomoea batatas*) cultivars. *International Journal of Biological Macromolecules, 189*, 758–767. https://doi.org/10.1016/j.ijbiomac.2021.08.106

Truong, V. D., Avula, R. Y., Pecota, K. V., & Yencho, G. C. (2018). Sweetpotato production, processing, and nutritional quality. In M. Siddiq, & M. A. Uebersax (Eds.), *Handbook of vegetables and vegetable processing* (2nd ed., pp. 811–838). John Wiley & Sons Ltd.. https://doi.org/10.1002/9781119098935.ch35

Tu, D. B., Jiang, Y., Salah, A., Xi, M., Cai, M. L., Cheng, B., … Wu, W. E. (2023). Variation of rice starch structure and physicochemical properties in response to high natural temperature during the reproductive stage. *Frontiers in Plant Science, 14*, 1136347. https://doi.org/10.3389/fpls.2023.1136347

Wei, C., Qin, F., Zhou, W., Yu, H., Xu, B., Chen, C., Zhu, L., Wang, Y., Gu, M., & Liu, Q. (2010). Granule structure and distribution of allomorphs in C-type high-amylose rice starch granule modified by antisense RNA inhibition of starch branching enzyme. *Journal of Agricultural and Food Chemistry, 58*, 11946–11954. https://doi.org/10.1021/jf103412d

Xu, J., Blennow, A., Li, X., Chen, L., & Liu, X. (2020). Gelatinization dynamics of starch in dependence of its lamellar structure, crystalline polymorphs and amylose content. *Carbohydrate Polymers, 229*, Article 115481. https://doi.org/10.1016/j.carbpol.2019.115481

Yang, H., Wei, Q., Lu, W., & Lu, D. (2021). Effects of post–silking low temperature on the physicochemical properties of waxy maize starch. *International Journal of Biological Macromolecules, 188*, 160–168. https://doi.org/10.1016/j.ijbiomac.2021.07.171

Yuryev, V. P., Krivandin, A. V., Kiseleva, V. I., Wasserman, L. A., Genkina, N. K., Fornal, J., … Schiraldi, A. (2004). Structural parameters of amylopectin clusters and semicrystalline growth rings in wheat starches with different amylose content. *Carbohydrate Research, 339*, 2683–2691. https://doi.org/10.1016/j.carres.2004.09005

Zhang, C., Yang, Y., Chen, Z., Chen, F., Pan, L., Lu, Y., Li, Q., Fan, X., Sun, Z., & Liu, Q. (2020). Characteristics of grain physicochemical properties and the starch structure in rice carrying a mutated *ALK/SSIIa* gene. *Journal of Agricultural and Food Chemistry, 68*, 13950–13959. https://doi.org/10.1021/acs.jafc.0c01471

Zhong, Y., Li, Z., Qu, J., Bertoft, E., Li, M., Zhu, F., Blennow, A., & Liu, X. (2021). Relationship between molecular structure and lamellar and crystalline structure of rice starch. *Carbohydrate Polymers, 258*, Article 117616. https://doi.org/10.1016/j.carbpol.2021.117616

Zhu, F., Yang, X., Cai, Y. Z., Bertoft, E., & Corke, H. (2011). Physicochemical properties of sweetpotato starch. *Starch, 63*, 249–259. https://doi.org/10.1002/star.201000134